Chinese Chemical Letters 33 (2022) 2096–2100

Contents lists available at ScienceDirect

Chinese Chemical Letters

journal homepage: www.elsevier.com/locate/cclet

A cellular chip-MS system for investigation of *Lactobacillus rhamnosus* GG and irinotecan synergistic effects on colorectal cancer

Wanting Hu[a,b], Dan Gao[a,*], Zhaochen Su[a], Rui Qian[a], Yu Wang[b], Qionglin Liang[b,*]

[a] State Key Laboratory of Chemical Oncogenomics, the Graduate School at Shenzhen, Tsinghua University, Shenzhen 518055, China
[b] Department of Chemistry, Center for Synthetic and Systems Biology, Key Laboratory of Bioorganic Phosphorus Chemistry & Chemical Biology (Ministry of Education), Tsinghua University, Beijing 100084, China

ARTICLE INFO

Article history:
Received 16 May 2021
Revised 20 July 2021
Accepted 8 August 2021
Available online 12 August 2021

Keywords:
Irinotecan
Lactobacillus rhamnosus
Microfluidics
Mass spectrometry
Colorectal cancer

ABSTRACT

Colorectal cancer (CRC) is still the leading cause of cancer death worldwide, but the clinical effect of drug therapy such as irinotecan is not an ideal way at present. In recent years, probiotics have attracted much attention, and the combination of probiotics may play an important role in the prevention and treatment of CRC. This work proposed a cellular chip-MS system, to study the synergistic effects of probiotic *Lactobacillus rhamnosus* GG (L.GG) and irinotecan on HCT116 cells by cell viability and on-line mass spectrometry (MS) analysis. The double-layer chip sandwiched with a polycarbonate membrane can co-culture HCT116 cells and L.GG. And the solid phase microextraction chip can be used for desalination and concentration. Finally, the extracted chemicals were entered the electrospray ionization quadrupole time-of-flight MS to detect irinotecan metabolites. The results showed that with the increasing concentration of co-cultured L.GG, the percentage of living HCT116 cells decreased, but the relative amount of metabolized SN-38 by HCT116 cells increased. Therefore, the microfluidic system can be used to detect and monitor the synergistic effect of irinotecan-L.GG combination on HCT116 cells. In summary, our study provided experimental evidence for the first time with potential applications of irinotecan-L.GG combination in CRC treatment, and the cellular chip-MS system as a powerful tool can be used in the experiments of probiotics as new drugs.

Colorectal cancer (CRC), also known as colon cancer, is still a serious health problem worldwide. It is a common malignant tumor in the gastrointestinal tract and one of the main causes of cancer death in the world [1]. In 2020, there were more than 1.9 million new (including anus) cases and 935,000 deaths all over the world [2]. In the general treatment of CRC, surgery, radiotherapy and chemotherapy are commonly used. Chemotherapy drugs commonly used for CRC include irinotecan, 5-fluorouracil, oxaliplatin and others. Unfortunately, due to the lack of effective treatment, adverse side effects, chemical resistance and disease recurrence of the current treatment methods, there is an urgent need to develop new therapeutic strategies for CRC.

The gut microbiota (including bacteria, archaea, viruses, fungi, protozoa and other microbes) has a profound impact on our overall health and response to disease [3]. And there is compelling evidence that the study of microbiota is important [4,5]. Probiotics are defined as foods containing living microorganisms that have a beneficial effect on the health of the host [6]. Experimental and clinical evidence suggest that probiotics may play an important role in a variety of human diseases, including CRC, inflammatory bowel disease, respiratory tract infection [7,8]. Nowadays, the strategy of implanting effective prebiotics, probiotics and derived epigenetic bacteria to improve the disease has been proposed in clinics [9], because intestinal flora may regulate the host response to clinical medication. Preclinical studies showed that *L. rhamnosus* (Lcr35) can decrease the severity of intestinal mucositis and diarrhea caused by adjuvant 5-FU-based chemotherapy in mice injected with CT26 colorectal adenocarcinoma cells [10]. Therefore, combinations of probiotics are considered to be a potential strategy for the prevention and treatment of CRC.

Microfluidic chip has great potential for the investigation of basic mechanisms in biology and toxicity [11–13]. It can establish a chemical or biological laboratory on several square centimeter chips, and integrate multiple functional units like cell culture, sorting, lysis and detection [14,15]. Moreover, microfluidic chip has many advantages, such as low cost, low reagent consumption, real-time and fast analysis of samples. Therefore, the microfluidic chip provides an alternative method for the establishment of a routine

* Corresponding authors.
E-mail addresses: gao.dan@sz.tsinghua.edu.cn (D. Gao), liangql@tsinghua.edu.cn (Q. Liang).

https://doi.org/10.1016/j.cclet.2021.08.041
1001-8417/

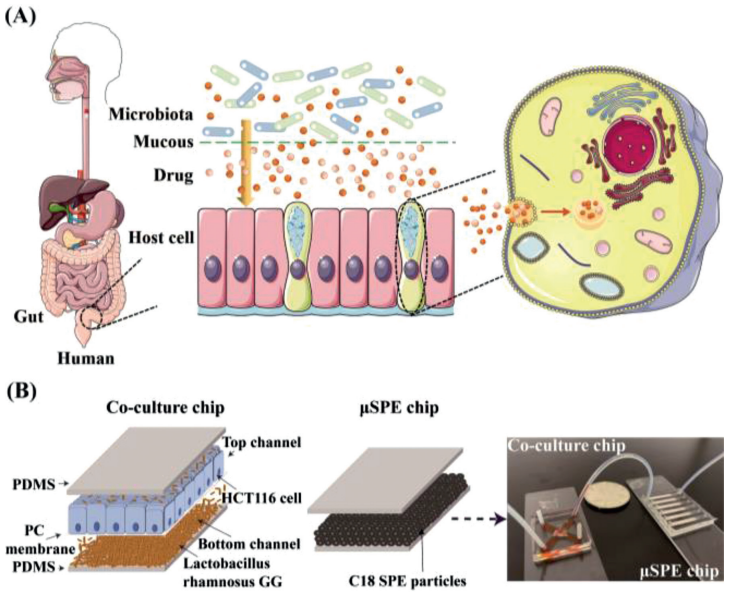

Fig. 1. (A) The pharmacokinetic process of the drug in the intestinal tract *in vivo* model. (B) The microfluidic system for co-culture of HCT116 cells with L.GG and metabolism detection.

preclinical model for drug screening [16–18]. The co-culture of probiotics and tumor cells on the microfluidic chip and the development of gut-on-chip makes it possible to study the combination therapy of CRC with probiotics and drugs [19–23]. Mass spectrometry (MS) is an ideal label-free analytical technique for analyzing the molecular composition with high sensitivity. In recent years, the improvement of the interface between microfluidic chips and MS allows rapid detection and analysis of cell metabolites [23–25]. These models may play important roles in exploring biological mechanisms that control pathological abnormalities observed in cancer. They will also serve as a more reliable platform for evaluating the predicted results of chemotherapeutics and their delivery systems *in vivo* [26].

In a real human environment, drugs must pass through the intestinal flora and across the intestinal mucosa before they can be absorbed and metabolized by intestinal cells (Fig. 1A). Here, we proposed a microfluidic system, which consists of two separate chips to study effects of *Lactobacillus rhamnosus* GG (L.GG) combined with irinotecan simultaneously on human colorectal cancer cell line HCT116 cells by electrospray ionization quadrupole time-of-flight MS (ESI-Q-TOF-MS) (Fig. 1B). One chip was a porous membrane sandwiched chip, which was used for co-culture of bacteria and HCT116 cells. Each channel was 18 mm long, 2 mm wide and 120 μm high. The porous polycarbonate (PC) membrane with a thickness of 10 μm and pores diameter of 0.4 μm was used to separate the top and bottom channels. As shown in Fig. S1 (Supporting information), the PC membrane was treated with 5% APTES for 20 min at 80 °C and 330 μg/mL matrigel for 40 min at 37 °C. The pores were still clearly visible under a scanning electron microscope (SEM), which could be used for next experiments. HCT116 cells were cultured in the top channel and L.GG were cultured in the bottom channel. To some extent, the direct contact of L.GG with HCT116 cells was restricted, but the penetration of L.GG through the PC membrane was not completely prevented. This design can ensure the good growth of both cells and L.GG. Irinotecan was added to both the top and bottom channels to stimulate cells. A home-made plug was applied when necessary, to ensure that different substances can be added to the top and bottom channels. The other chip was a solid phase microextraction (μSPE) chip with the channel length of 22 mm, width of 2 mm, height of 80 μm, and micro-column arrays at the end with 30 μm intervals, which was used for the extraction and concentration of cell culture medium and metabolites. C18 SPE materials were employed to desalinate and enrich the metabolites of irinotecan. After concentration and extraction, the μSPE chip was directly connected to ESI-Q-TOF-MS through polytetrafluoroethylene (PTFE) tubes for metabolites analysis. Our established system provided a powerful tool to study cell metabolism and anti-cancer drug screening.

HCT116 cells at 5×10^6 cells/mL were seeded into the top channel, and then the microfluidic device was placed in a 10 cm diameter dish to keep sterile, and cultured in 5% CO_2 and 95% air at 37 °C. Due to the permeability of PDMS, the cell culture medium in the channel was easy to evaporate after a few hours. To reduce evaporation, the surface of the chip was covered with a layer of cell culture medium. After this treatment, no evaporation was observed in the channel for several days. To ensure that our established system had no effect on the cell viability, a Live/Dead assay kit composed of Calcein AM and ethidium homodimer-1 (EthD-1) was used for cell viability evaluation. As shown in Fig. S2 (Supporting Information), cells on the chip were completely spread out and attached to the PDMS. On the first, third, and fifth day, nearly 100% of cells remained alive and showed bright green fluorescence.

CCK-8 was used to evaluate the cytotoxicity of irinotecan on HCT116 cells. As shown in Fig. S3 (Supporting information), the survival rate of HCT116 cells decreased with irinotecan final concentrations increasing from 3.81 μmol/L to 61.00 μmol/L in using two-fold dilutions, and the IC_{50} value was 10.61 μmol/L. To keep appropriate live cells for the following combination study of probiotics and drugs on HCT116 cells, the IC_{50} value of irinotecan was used for further experiments.

Before investigating the effect of L.GG on the proliferation of HCT116 cells, basic properties like morphology and growth ability were tested. For growth curve evaluation, an optical density of L.GG at 600 nm (OD_{600}) was measured instead of testing the number of viable bacteria each time. The growth curve was measured as follows, L.GG with OD_{600} 0.07 was cultured in a 15 mL centrifuge tube and measured the density change every 3 h lasting for 48 h. As shown in Fig. S4A (Supporting information), OD_{600} was increased relatively fast during 33 h culture and then became flat. The corresponding quantification result between OD_{600}

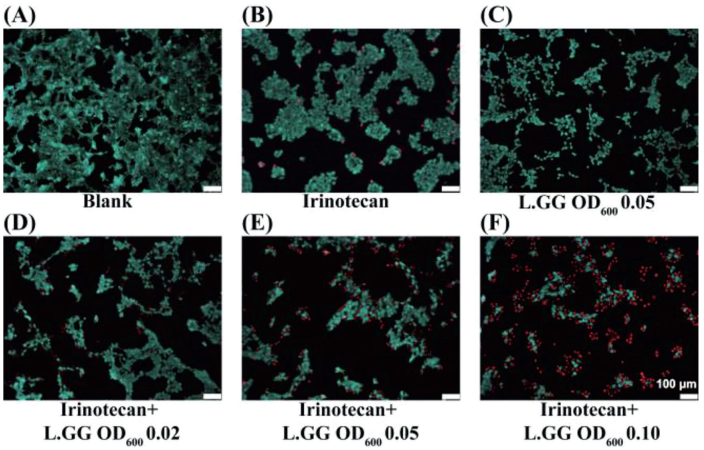

Fig. 2. HCT116 cells viability assay with a Live/Dead assay kit after treated with 10.61 μmol/L irinotecan, L.GG, or their combinations. (A) Without any treatment. (B) Only treated with 10.61 μmol/L irinotecan. (C) Only treated with L.GG of OD_{600} 0.05. Simultaneously treated with 10.61 μmol/L irinotecan and L.GG with OD_{600} (D) 0.02, (E) 0.05, and (F) 0.10. All the scale bars were 100 μm.

and CFU/mL was shown in Fig. S4B (Supporting information). It was found that there was a good linear relationship between OD_{600} and CFU/mL. The fitting formula was $y = 2.0806x + 6.8869$, $R^2 = 0.9960$. Results indicated that the good proliferation ability of L.GG *in vitro* was helpful for the subsequent effect on the viability of tumor cells. Moreover, an SEM was employed to characterize the morphology of L.GG. As Figs. S4C and D (Supporting Information), L.GG presented a rod-shaped structure.

Six different experimental groups were set up to explore the combined effect of irinotecan and L.GG on HCT116 cells. Firstly, 5×10^6 cells/mL HCT116 cells were added to the top channel. After 24 h culture, the original medium was removed, and 10.61 μmol/L irinotecan dissolved in culture medium was added to the top channel to treat cells. Meanwhile, irinotecan of 10.61 μmol/L dissolved in culture medium containing increasing concentrations of L.GG with OD_{600} from 0.02 to 0.10 was added to the bottom channel. HCT116 cells without any treatment was regarded as blank (Fig. 2A). While HCT116 cells treated only with 10.61 μmol/L irinotecan (Fig. 2B) or L.GG with OD_{600} 0.05 (corresponding to about 9.79×10^6 CFU/mL in bacteria concentration) were used as control groups. After 48 h treatment, all the cell medium were loaded on the activated μSPE chip at a flow rate of 1 μL/min for desalination and concentration. The Live/Dead assay kit was then used to evaluate the cell viability on the chip. As shown in Fig. 2, compared with the blank, the cell proliferation was significantly reduced when cells were treated with 10.61 μmol/L irinotecan and L.GG with OD_{600} 0.05. HCT116 cells were liable to aggregate growth. However, when they were co-cultured with L.GG, the cells were tended to disperse (Fig. 2C). As shown in Figs. 2D–F, with the increased concentration of co-cultured L.GG, viable HCT116 cells decreased and apoptotic cells increased. Results indicated that L.GG and irinotecan had a synergistic effect on the inhibition of HCT116 cells growth.

In order to analysis cellular metabolites, μSPE chip was designed to desalt and concentrate the metabolites before ESI-Q-TOF-MS analysis. This method has the advantages of fast, convenient, high throughput and high sensitivity. The unique polymer beads of C18 extraction were selected as packing materials for desalting and adsorbing irinotecan and its metabolites. The filling effect of μSPE chips was shown in Fig. S5 (Supporting information). C18 SPE particles were tightly filled in the microchannels which can be used for subsequent experiments.

MRM mode was used to detect MS and the tandem mass spectrometry (MS/MS) of irinotecan and SN-38 simultaneously. As shown in Fig. S6 (Supporting information), the detection of 5.01 μmol/L irinotecan containing 0.3% formic acid did not contain 393.14 fragments deducting background effects under optimal MS conditions used in this experiment.

Irinotecan of 61.00 μmol/L and its metabolites SN-38 of 10.70 μmol/L were dissolved in phosphate buffered saline (PBS), serially diluted in PBS. The final concentration of irinotecan reached from 0.95 to 61.00 μmol/L, and the final concentration of SN-38 reached from 0.08 to 10.70 μmol/L. These solutions were extracted by μSPE chip separately, and finally detected online by ESI-Q-TOF-MS under optimal MS conditions. Moreover, MS/MS was used to verify their chemical structures. As shown in Figs. S7A and B (Supporting information), the ion intensities of the monitored ions increased with the increasing concentration of irinotecan or SN-38. And there were good linear relationships between the logarithm of the highest intensity generated from *m/z* 587.28 peaks and the logarithm of the irinotecan concentration, and the logarithm of the highest intensity generated from *m/z* 393.14 peaks and the logarithm of the SN-38 concentration, separately. The calibration curve of irinotecan was linear in the range of 0.95–61.00 μmol/L, and the fitting formula was $y = 0.9028x + 4.8331$, $R^2 = 0.99534$. The calibration curve of SN-38 was linear in the range of 0.08–10.70 μmol/L, and the fitting formula was $y = 0.9065x + 3.4356$, $R^2 = 0.99446$. All the above results indicated that the established μSPE chip and ESI-Q-TOF-MS combination system could be used for irinotecan and its metabolite SN-38 characterization and semi-quantification analysis.

After HCT116 cells were co-cultured with L.GG and treated with 10.61 μmol/L irinotecan simultaneously, the culture medium was extracted by μSPE chip and analyzed by ESI-Q-TOF-MS. As shown in Fig. 3, the monitoring ions of *m/z* 587.28 and its fragments of *m/z* 543.29, *m/z* 502.19 and *m/z* 458.20 indicated the presence of irinotecan, while the monitoring ions of *m/z* 393.14 and the fragments of *m/z* 349.14 indicated the presence of SN-38. The whole online detection time was only about 7 min. Results showed that SN-38 can be effectively secreted into the medium and was the main metabolite of irinotecan in HCT116 cells, which was accordance with the findings reported in the previous literature [27].

HCT116 cells were co-cultured with three different concentrations of L.GG (OD_{600} 0.02, 0.05 and 0.10) and treated with 10.61 μmol/L irinotecan simultaneously. After 48 h treatment, the relative intensity of SN-38 increased significantly with the increasing concentration of L.GG, but the cell viability decreased markedly (Fig. 4). The results might be caused by the higher toxicity of SN-38 than irinotecan, which was in accordance with the findings reported in the previous literature [28]. We also investigated the effects of irinotecan-L.GG combination on HCT116 cells for 0, 24 and

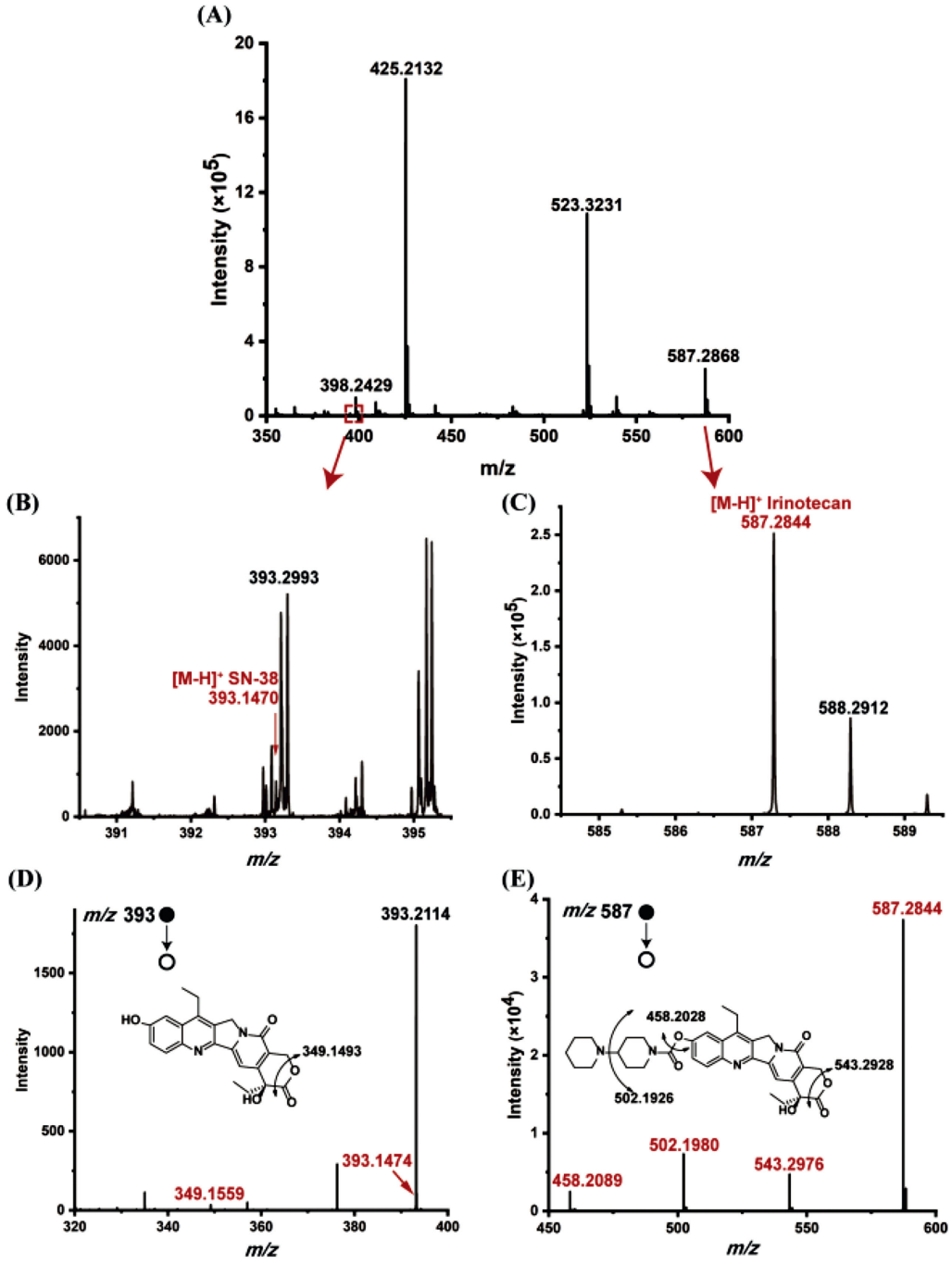

Fig. 3. (A) Mass spectra of cell medium from HCT116 cells incubated with 10.61 μmol/L irinotecan and L.GG with OD_{600} 0.10 for 48 h. Locally enlarged mass spectra of (B) SN-38 and (C) irinotecan, and their corresponding tandem mass spectra of (D) SN-38 and (E) irinotecan.

48 h separately, with the irinotecan of 10.61 μl/L and the L.GG of OD_{600} 0.05. As shown in Fig. S8 (Supporting information), the concentration of SN-38 in the medium has dramatically increased with the treatment time prolonged to 48 h. Therefore, these results suggested that L.GG can help the absorption of irinotecan by HCT116 cells and metabolize it to the main metabolite SN-38. These results proved the feasibility of using a cellular chip-MS system for cells and probiotics co-culture and drug metabolism study. Moreover, these results proved that the irinotecan-L.GG combination could improve the treatment efficiency for CRC.

In summary, we proposed a cellular chip-MS system, which consisted of two independent chips. Effects of irinotecan-L.GG combination on HCT116 cells was studied by the ESI-Q-TOF-MS. Here, when irinotecan-L.GG combination was used to treat HCT116 cells, with the increase of the L.GG concentration, the apoptosis of HCT116 cells was obvious, and SN-38, the main metabolite of irinotecan, was increased. Consequently, we demonstrated for the first time that irinotecan-L.GG combination can improve the treatment efficiency of colorectal cancer. Moreover, the cellular chip-MS system can be used as a highly sensitive detection method, which provided a powerful tool for the study of cell metabolism and anticancer drug screening, especially in the experiments of probiotics as new drugs.

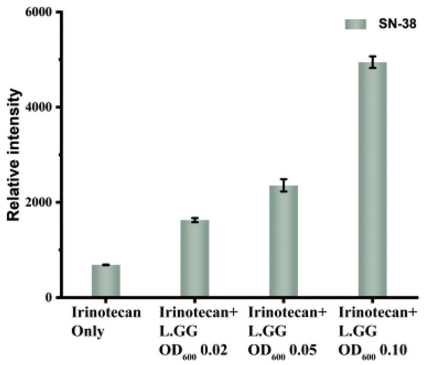

Fig. 4. Relative mass spectra signal intensities of SN-38 in the experimental group treated with the irinotecan-L.GG combination compared to that treated with irinotecan alone.

Declaration of competing interest

The authors declare that they have no known competing financial interests or personal relationships that could have appeared to influence the work reported in this paper.

Acknowledgments

This work was supported by the Natural Science Foundation of Guangdong Province, China (No. 2020A1515010660), Shenzhen Fundamental Research and Discipline Layout project (No.JCYJ20180508152244835), 1226 Engineering Health Major Project (Nos. BWS17J028, AWS16J018), and Research and Development Program in Key Areas of Guangdong Province, China (No. 2019B020209009).

Supplementary materials

Supplementary material associated with this article can be found, in the online version, at doi:10.1016/j.cclet.2021.08.041.

References

[1] S. Afrin, F. Giampieri, M. Gasparrini, et al., Biotechnol. Adv. 38 (2020) 107322.
[2] H. Sung, J. Ferlay, R. Siegel, et al., CA Cancer J. Clin. 0 (2021) 1–41.
[3] B. Helmink, M. Khan, A. Hermann, et al., Nat. Med. 25 (2019) 377–388.
[4] M. Wilson, Y. Jiang, P. Villalta, V. Gopalakrishnan, J. Wargo, Science 363 (2019) eaar7785.
[5] C. Gentile, T. Weir, Science 362 (2018) 776–780.
[6] S. Salminen, C. Bouley, M. Boutron-Ruault, et al., Br. J. Nutr. 80 (1998) S147–S171.
[7] R.G. Kerry, J. Patra, S. Gouda, et al., J. Food Drug Anal. 26 (2018) 927–939.
[8] C. Chang, C. Liu, H. Lee, et al., Front Microbiol. 9 (2018) 983.
[9] Y. Tsai, T. Lin, C. Chang, et al., J. Biomed. Sci. 26 (2019) 3.
[10] C.Amoroso F.Perillo, F. Strati, et al., Int. J. Mol. Sci. 21 (2020) 5389.
[11] H. Shi, K. Nie, B. Dong, et al., Chem. Eng. J. 361 (2019) 635–650.
[12] Y. Ai, F. Zhang, C. Wang, R. Xie, Q. Liang, TrAC Trend Anal. Chem. 117 (2019) 215–230.
[13] F. Zhang, D. Gao, Q. Liang, Chin. J. Anal. Chem. 44 (2016) 1942–1949.
[14] R. Pol, F. Céspedes, D. Gabriel, M. Baeza, TrAC Trend Anal. Chem. 95 (2017) 62–68.
[15] X. Ai, Q. Liang, M. Luo, et al., Lab Chip 12 (2012) 4516–4522.
[16] B. Zhang, A. Korolj, B. Lai, M. Radisic, Nat. Rev. Mater. 3 (2018) 257–278.
[17] M. Rothbauer, J. Rosser, H. Zirath, et al., Curr. Opin. Biotechnol. 55 (2019) 81–86.
[18] S. Feng, S. Mao, Q. Zhang, W. Li, J. Lin, ACS Sens. 4 (2019) 521–527.
[19] Y. Wang, Z. Shao, W. Zheng, et al., Biofabrication 11 (2019) 045001.
[20] D. Gao, H. Liu, G. Guo, J. Lin, Lab Chip 13 (2013) 978–985.
[21] P. Shah, J.V. Fritz, E. Glaab, et al., Nat. Commun. 7 (2016) 11535.
[22] S. Jalili-Firoozinezhad, F. Gazzaniga, E. Calamari, et al., Nat. Biomed. Eng. 3 (2019) 520–531.
[23] L. Lin, Y. Zheng, Z. Wu, W. Zhang, J. Lin, Chem. Commun. 55 (2019) 10218–10221.
[24] S. Mao, W. Li, Q. Zhang, et al., TrAC Trend Anal. Chem. 107 (2018) 43–59.
[25] D. Gao, H. Wei, G. Guo, J. Lin, Anal. Chem. 82 (2010) 5679–5685.
[26] L. Mathur, M. Ballinger, R. Utharala, C. Merten, Small 16 (2020) e1904321.
[27] M. Sun, X. Tian, Z. Yang, Anal. Chem. 89 (2017) 9069–9076.
[28] J. Fuscoe, V. Vijay, J. Hanig, et al., Clin. Cancer Res. 7 (2001) 2182–2194.